Integrative Biology

Accepted Manuscript

ROYAL SOCIETY OF CHEMISTRY

www.rsc.org/ibiology

Insight statement:

Abnormal interactions of Aβ with Zn^{2+} and Cu^{2+} are proposed to play an important role in the neuropathogenesis of AD. Therefore, modulating metal–Aβ interaction is an effective method to inhibit the Aβ aggregation and depress the neurotoxicity. In this study, two cyclam derivatives were chosen to study their ability to modulate metal-mediated A*β* events. From two aspects of the prevention and treatment of AD, the effects and biological activities of the chelators were evaluated at both molecular and cellular levels by the means of chemical and biological methods, which is the innovation point of this work. The action mechanisms of chelators were also discussed. These would lay the solid foundation for the evaluation and development of anti-AD drugs.

Cite this: DOI: 10.1039/c0xx00000x

ARTICLE TYPE

www.rsc.org/xxxxxx

Two macrocyclic polyamines as modulators of metal-mediated Aβ_{40} aggregation

Yanfei Yang[b], Tingting Chen[a,b*] Shajun Zhu[c], Xuefang Gu[a], Xueping Jia[a], Yapeng Lu[b], Li Zhu[b,d*]

Received (in XXX, XXX) Xth XXXXXXXXX 20XX, Accepted Xth XXXXXXXXX 20XX

DOI: 10.1039/b000000x

Dysfunctional interactions of amyloid-β (Aβ) with Zn and Cu ions are proved to be related to the etiology of Alzheimer's disease (AD). Disruption of these metal-Aβ interactions using metal chelators holds considerable promises as a therapeutic strategy to combat this incurable disease. Herein, we report that two cyclam derivatives (L1 and L2) are capable of modulating Zn^{2+}/Cu^{2+}-mediated Aβ_{40} aggregation, reactive oxygen species (ROS) production, and neurotoxicity. These chelators were found to inhibit the metal-induced Aβ aggregation, dissociate metal-Aβ aggregates and restore metal-induced β-sheet structure of Aβ_{40} to its random coil conformation, as observed by BCA protein assay, thioflavin T fluorescence and circular dichroism spectroscopy. Moreover, preliminary investigation on SH-SY5Y cells indicates that L1 and L2 can diminish the neurotoxicity of metal-Aβ species, control metal-Aβ-triggered ROS production and protect cells against apoptosis. These observations warrant the further investigations on L1 and L2 as potential anti-AD agents.

1. Introduction

Alzheimer's disease (AD), a progressive, chronic and fatal neurodegenerative disorder characterized by memory loss, cognitive impairment and decline in language, affects older people all over the world.[1] Development of a cure for AD has been hindered by a lack of understanding of both the causes and mechanisms of disease onset and progression.[2-5] The major pathological hallmarks of AD are extracellular amyloid plaques, the major component of which is the amyloid-β (Aβ) peptide and intracellular neurofibrillary tangles composed of hyper-phosphorylated forms of the microtubule associated protein called tau.[2, 6-8] The main alloforms of the Aβ peptide, Aβ_{40} and Aβ_{42}, present in the brain at ca. 90 % and 9 %, respectively, are primarily produced upon cleavage of amyloid precursor protein (APP) by β- and γ-secretases.[2-5] According to the amyloid cascade hypothesis, the increased production and accumulation of the Aβ peptide promote the formation of Aβ oligomers, protofibrils, and ultimately amyloid fibrils that lead to neurogeneration.[9, 10] Although Aβ is proposed to be a causative factor in AD, a relationship between specific peptide oligomers and toxicity remains unclear despite recent findings indicating soluble Aβ oligomers are possible neurotoxic species.[11-14]

Apart from an imbalance between the production and clearance of Aβ peptides, remarkably high levels of metal ions (Zn, 1055 μM; Cu, 390 μM, Fe, 940 μM) have been found within the amyloid deposits in AD-affected brains tissue compared to healthy tissue,[4,5,11,15] and several studies have investigated the interactions of metal ions with monomeric Aβ peptides and their correlation with amyloid plaque formation.[15-20] These metal ions particularly Zn and Cu, bind to Aβ peptides facilitating their aggregation.[6, 7, 15-19, 21, 22] Furthermore, these metal ions are implicated in the formation of reactive oxygen species (ROS) in Aβ pathology.[21, 23, 24] Moreover, dysregulated redox active metal ions, Cu and Fe, both unbound and bound to Aβ, are observed to promote overproduction of reactive oxygen species (ROS) via Fenton chemical reactions giving rise to oxidative stress, thus resulting in AD progression.[25-27] Although the detailed interaction mechanism of the metal ions with Aβ is still unclear, it is generally accepted that the metal ions can coordinate with Aβ at N-terminal residues, such as His6, His13, and His14 imidazole and the carbonyl groups, and in turn promote the aggregation of Aβ[21, 28, 29].

Metal chelators have been considered as potential therapeutic candidates, partly due to the metal ion hypothesis, and the possible contribution of metal-Aβ to AD.[30] Using traditional metal chelating agents, potential regualtion of metal-induced Aβ aggregation and neurotoxicity has been shown in vitro and in vivo.[7, 21, 31-34] Several chelators such as desferrioxamine (DFO), clioquinol (CQ) and an 8-hydroxyquinoline derivative (PBT2) have been tested in murine AD models and AD patients.[1, 2, 21] CQ has been shown to dissolve Alzheimer-like amyloid deposits in transgenic mice and in some cases to slow the cognitive decline associated with AD.[35, 36] PBT2 has been shown to lower levels of Aβ_{42} in the CSF of AD patients without affecting serum metal ion levels (Zn^{2+}, Cu^{2+}).[37] All these compouds have yielded promising results, however the potential side effects of these metal chelators may prohibit their widespread clinical use. For example, long-term use of CQ is limited by an adverse side effect, subacute

myelo-optic neuropathy.[38, 39] Although these traditional chelators have yet to be available as effective therapeutic agents, the studies provide a useful direction to search the possible chelators in the further research. Thus, our work presented herein demonstrate the value of macrocyclic polyamines compounds which are considered as potential agents for investigating metal-Aβ-involved events due to their coordination with metal ions toward metal-Aβ species.

Macrocyclic chelators are important polyamines, and metal complexes of their derivatives have many in vivo applications in medicinal chemistry as diagnostic imaging and/or therapeutic agents because macrocyclic polyamines have strong affinity with kinetically inertness and thermodynamically stability. Their selective binding to certain metals and facile functionalization at the N position promote their use for in vivo applications in medicinal chemistry as diagnostic imaging and/or therapeutic agents. They have properties of low molecular weight, poor or noncharged form and amphiphilic solubility, which are beneficial for crossing the blood-brain barrier(BBB).[40] Overall, these beneficial features prompted the study of tetraazamacrocycles as metal-binding agents for the treatment of AD. Our previous studies have shown that tetraazamacrocycles can effectively inhibit the metal-induced Aβ aggregation.[33] In addition, Green and coworkers have reported that the pyridine backbone of chelator engenders antioxidant and protective capacity against ROS induced cell death in AD.[41]

Based on these above researches, pyridine groups were introduced to the scaffold of 1,4,8,11-tetrazacyclotetradecane in order to enhance their antioxidant activity, without affecting the metal ion chelation capability. Moreover, hydrophobic substituents such as two methyl and (N-(2-(pyridin-2-yl)ethyl)acetamide groups can increase the lipophilicity of 1,4,8,11-tetrazacyclotetradecane, which may be helpful for chelators to pass through the BBB. This work focuses on the use of 2-(4,11-dimethyl-1,4,8,11-tetraazacyclotetradecan-1-yl)-N-(2-(pyridin-2-yl)ethyl)acetamide (L1) and 2,2'-(4,11-dimethyl-1,4,8,11-tetraazacyclotetradecane-1,8-diyl)bis(N-(2-(pyridin-2-yl)ethyl)acetamide) (L2) shown in Figure 1 as metal ion passivation and antioxidant agents. Here, we report the capacity of L1 and L2 to modulate metal-mediated Aβ_{40} aggregation pathway. As expected, both chelators can inhibit Zn^{2+}- or Cu^{2+}-induced Aβ_{40} aggregation, suppress the intracellular ROS production, and palliate neurotoxicity.

2. Materials and methods

2.1 Materials and reagents

Human Aβ_{40} was purchased from GL Biochem Ltd.(Shanghai, China) and verified by high-performance liquid chromatography and electrospray ionization mass spectrometry (ESI-MS). Zinc acetate dehydrate, copper chloride, thioflavin T (ThT), 2′,7′-dichlorofluorescin diacetate (DCFH-DA), horseradish peroxidase (HRP) and tris(hydromethyl)aminomethane (Tris) were purchased from Sigma-Aldrich. L1 and L2 were synthesized according to the literature methods.[42] Other common reagents used in the experiments were all of analytical grade. Stock solutions of Aβ_{40}, Zn^{2+} and Cu^{2+} were prepared according to the reported procedure.[36] those of L1 and L2 were prepared by dissolving each compound in water to give a final concentration of 4 mM. All the aqueous solutions used in this study were prepared with Milli-Q water and filtered through a 0.22 μm filter (Millipore).

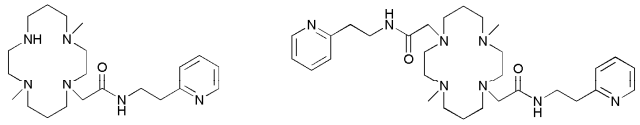

Fig. 1 The structure of L1 and L2

2.2 BCA Protein Assay

The samples (100 μL) consisting of Aβ_{40} (40 μM), $Zn(Ac)_2$ or $CuCl_2$(80 μM) was incubated at 37 ˚C. In inhibition assay, treatment of Aβ_{40} with metal or metal free for 2 min first, then L1 or L2 (160 μM) was added to metal-Aβ_{40} solution followed by incubation at 37 ˚C for 24 h. While in disaggregation assay, Aβ_{40} incubated with metal or metal free at 37 ˚C. After 24 h, L1 and L2 were added to the prepared metal-Aβ_{40} samples for another incubation of 24h. Final, the absorption of each sample in BCA protein assays were examined at absorption wavelength of 405 nm by a multifunctional microplate reader (BioTek Synergy2).

2.3 Thioflavin T Fluorescence

The aggregations of Aβ_{40} were detected by ThT fluorescence. In inhibition assay，L1 or L2 (80 μM) was added to the sample of Aβ_{40} (20 μM) in the absence and presence of Zn^{2+}/Cu^{2+} (40 μM) followed by incubation at 37 ℃ for 24 h. For the disaggregation studies, Aβ_{40} (20 μM) with and without Zn^{2+}/Cu^{2+} (40 μM) was incubated for 24 h at 37 ℃ before the addition of L1 or L2 (80 μM) to the sample. The resulting samples were incubated at 37 ℃ for another 24 h. After incubation, each sample was treated with ThT, and shaking for 5 min in the dark. The final concentration of ThT was 10 μM. Fluorescence signal was measured (excitation wavelength 415 nm) on a fluorescence spectra (SHIMADZU, RF-5301pc, Japan), and an average of three scans was regarded as the final result.

2.4 Circular Dichroism (CD) Measurement

Sample solutions were prepared freshly in a phosphate buffer (5 mM, pH 7.4) containing either Aβ_{40} (50 μM) alone or with Zn^{2+}/Cu^{2+}(100 μM) which were kept in a incubator at 37˚C for 24h. L1 or L2 (200 μM) was added to each solution and then incubated for 12 h at 37 ˚C. CD measurements were carried out with a Chirascan spectrometer (Applied Photophysics Ltd., Leatherhead, Surrey, U.K.) controlled by the Jasco software and equipped with temperature control quantum. The spectra were recorded from 190 to 260 nm with a scan speed of 50 nm / min and a bandwidth of 1 nm using 0.1 cm quartz cells. The data of the baseline acquired in the absence of a peptide were subtracted from each spectrum.

2.5 H_2O_2 Detection

DCFH-DA stock solution (1 mM) was prepared in buffer (20 mM Tris-HCl/150 mM NaCl, pH 7.4) according to the reported procedures. Horseradish peroxidase (HRP) stock solution (4 μM) was prepared with the same buffer. Sample solutions containing Aβ_{40} (300 nM) and $CuCl_2$ (150 nM) were incubated with or without chelators (300 nM) at 37 ºC for 24h. Ascorbate (2 μM) was added to each sample and incubated for 2 min. HRP (0.03 μM) and DCFH-DA (100 μM) were added to each solution and incubated for 10 min in the dark at room temperature.

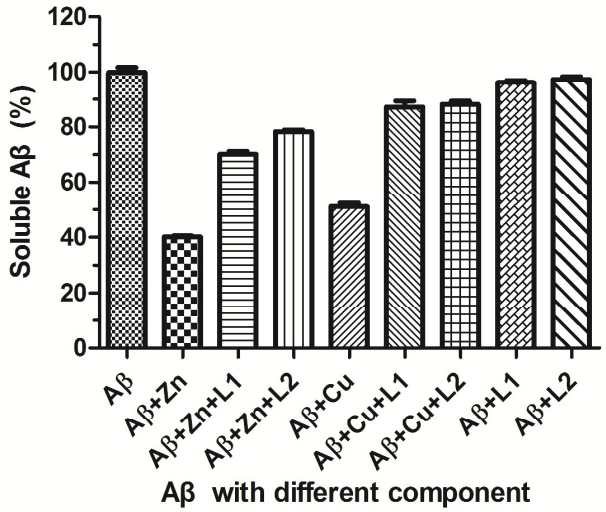

Fig. 2 Percentage of soluble Aβ_{40} (40μM) in the solution without or with Zn^{2+} or Cu^{2+} ions in the absence and presence of chelators after incubation at 37˚C and pH 7.4 for 24 h in inhibition assay ([Aβ_{40}] : [Cu^{2+}]/ [Zn^{2+}]: [L1]/ [L2] = 1 : 2 : 4]).

Fluorescence spectra (λ_{ex} = 485 nm) in the range of 490–650 nm were recorded by a fluorescence spectrophotometer (SHIMADZU, RF-5301pc, Japan).

2.6 Cell Culture

SH-SY5Y cell line (human neuroblastoma，Chinese Academy of Sciences， Shanghai, China) was cultured in Dulbecco's Modified Eagle Medium (DMEM)-F12 (HyClone) supplemented with 10 % (v/v) fetal bovine serum (FBS, HyClone), penicillin 100 U/mL and streptomycin 100 mg/mL (Invitrogen). The cells were grown at 37°C in a humidified atmosphere of 5 % CO_2.

2.7 MTT Assay

By cell counting, cells were seeded at a density of 3.5×10^4 per well in 100 μL on a 96 well plate. Based on various concentrations of chelators cytotoxicity experiments, Aβ_{40} (10 μM) alone or incubated with Zn^{2+} or Cu^{2+} (10 μM) in the presence or absence of L1 or L2 (20 μM). After 24 h, every well was treated with 0.5 mg/mL MTT (25 mg MTT in 5mL DMEM without FBS) for 4 h at 37 °C then adding double distilled water containing SDS (20 % (w/v)) to lysis overnight, at 37 °C in the dark. Using a multifunctional microplate reader (BioTek, Synergy2) to subsequently evaluate the degree of MTT reduction in each sample by measuring absorption at 570 nm at room temperature. The absorbance measured in an average of six wells and regarded as mean ± standard deviation (S.D.) percentage of cell viability. The data were normalized and calculated as a percentage of untreated vehicle control values.

2.8 Measurement of intracellular ROS

Intracellular ROS generation was measured by fluorescence microscopy upon staining with DCFH-DA. The cells were plated at a density of 3.5×10^4 per well in 100 μL on a 96 well plate in fresh medium. Aβ_{40} (10 μM) incubated with or without Zn^{2+} or Cu^{2+} (10 μM) in the presence or absence of L1 or L2 (20 μM) in SH-SH5Y cells for 24 h. Before staining treatment, the old medium was removed and the probe was diluting in FBS-free

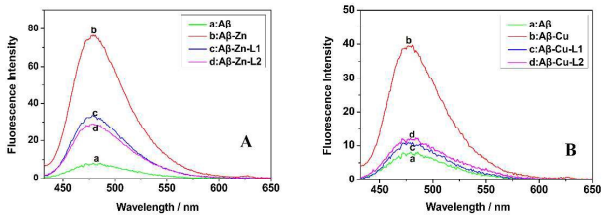

Fig. 3 ThT fluorescence spectra of Aβ_{40} (20 μM) solutions in the absence and prescence of Zn^{2+} (A) or Cu^{2+} (B) and L1 or L2 after incubation at 37˚C for 24 h in inhibition assay. ([Aβ_{40}] : [Cu^{2+}]/ [Zn^{2+}]: [L1]/ [L2] = 1 : 2 : 4]).

medium at 10 μM. Each sample was incubated with the probe for another 50 min in the dark. Then measured the DCF fluorescence intensity at emission wavelength of a range 525 nm and excitation wavelength of 485 nm by a microplate reader(BioTek, Synergy2).

2.9 Hoechst 33342 staining

SH-SY5Y cells were inoculated into holes with a density of 3.5×10^5 cells per well in total 500 μL on a 24 well plate which spread sterilized glass cover slips in every hole. Aβ_{40} (10 μM) alone or incubated with Zn^{2+} or Cu^{2+} (10 μM) in the presence or absence of L1 or L2 (20 μM) at 37 °C. After 24 h, exposing the sterilized glass to Hoechst33342 dye (Sigma, shanghai) to evaluate the morphology of apoptosis by fluorescence. Firstly, the cells on every glass coverslip were washed by PBS three times and fixed with 4 % paraformaldehyde. Then, using Hoechst 33342 (10 μg/mL) to stain 15 min in a dark chamber at room temperature and visualized in a fluorescence microscope (Leica DM4000, Germany) then photographed. Each sample was took pictures for three different views, then statistics the number of apoptosis and do statistical analysis. Morphology of nucleus is observed by fluorescence microscope. At last, about 100 nuclei were counted microscopically in every field.

2.10 Statistical Analysis

The experimental data were analyzed by Graph Pad Prism software through Single factor analysis of variance statistics followed Duke Cramer's post hoc comparison to determine the intermediate data set of significant. Significance was defined as $P < 0.05$.

3. Results and discussion

Change in Soluble Aβ Content

The effect of two chelators on inhibiting the Zn^{2+}- or Cu^{2+}-mediated Aβ_{40} aggregation was assessed by BCA protein assay firstly, a sophisticated approach investigating the percentage of soluble Aβ_{40} in the supernatant.[43] As Figure 2 shown, Aβ_{40} incubated alone was almost completely soluble. However soluble Aβ_{40} decreases to 40.1 % or 51.2 % of original Aβ_{40} amount after incubated with Zn^{2+} or Cu^{2+}. In the presence of L1 or L2, the content of soluble Aβ_{40} is largely increased. Through the statistical analysis, L1 or L2 with Zn^{2+}-Aβ_{40} system reaching 70.2 % and 78.2 %, respectively, and the Cu^{2+}-Aβ_{40} system reaching 87.3 % and 88.2 % compared with starting soluble Aβ_{40} amount, respectively. The results demonstrate that

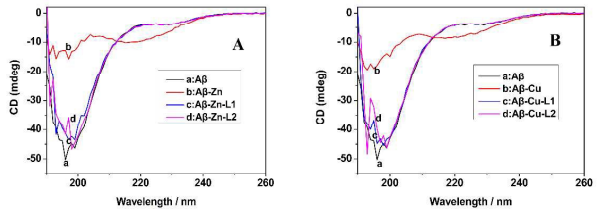

Fig. 4 Circular dichroism spectra of Aβ_{40} alone or in the prescence of Zn^{2+} (A) or Cu^{2+} (B) before and after addition of L1 or L2 at 37 ˚C ([Aβ_{40}]= 50 μM; [Aβ_{40}] : [Cu^{2+}]/ [Zn^{2+}]: [L1]/ [L2] = 1 : 2 : 4).

L1 and L2 can effectively inhibit the metal-induced aggregation of Aβ_{40}. The solubilization effect of L2 appears to be slightly stronger than that of L1 for the Zn^{2+}-induced Aβ_{40} accumulation, while the difference is not apparent for the Cu^{2+}-induced accumulation. Additionally, the disaggregation assay was also conducted to assess the ability of L1 and L2 to disassemble preformed metal-associated Aβ_{40} aggregates. The disaggregation assay was performed as follow: first, Aβ_{40} incubated alone or with metal ions for 24 h, then L1 or L2 was added to metal-Aβ_{40} samples, which is different from the inhibition assay. As shown in Figure S1, Our disaggregation assay result indicated that L1 and L2 could disassemble metal-Aβ_{40} aggregates. L1 and L2 with Zn^{2+}-Aβ_{40} system reversed from 40.2 % to 70.2 % and 78.2 %, and the similar results of Cu^{2+}-Aβ_{40} system treated with L1 and L2 increased from 51.2 % to 87.3 % and 88.2 %, respectively. As presented in Figure 2, in the presence of L1 or L2, the percentage of soluble Aβ_{40} is about 97.4 %, so the change of soluble Aβ_{40} content may mainly arise from the chelation of L1/L2 and metal ions.

Influence of L1 and L2 on *β*-aggregation

The aggregation degrees of Aβ_{40} with different additives were examined by ThT fluorescence assay. ThT specifically binds to the *β*-sheet of amyloid beta rapidly but not to monomers nor oligomers. Therefore the fluorescence intensity at 480 nm could be used to quantify A*β* fibrils.[44,45] As clearly shown in Figure 3, Aβ_{40} incubated at 37 ºC in the absence of Zn^{2+} or Cu^{2+} showed a slight increase in fluorescence intensity, indicating that the amount of *β*-aggreagtes is very limited. In the presence of Zn^{2+} or Cu^{2+}, Aβ_{40} showed a significant increase in fluorescence signal, suggesting considerable amount of *β*-aggreagtes is formed, which is in line with the previous research. When L1 or L2 was added to the solution of Zn^{2+}- or Cu^{2+}-Aβ_{40}, a large decrease in fluorescence was observed, which indicated that L1 or L2 can inhibit the Zn^{2+}- and Cu^{2+}-induced *β*-aggregation of Aβ_{40}. The same effect was obtained in disaggregation assay showing that L1 and L2 can diminish the formation of *β*-aggreagtes (Figure S2).Therefore, according to the detection of ThT fluorescence in inhibition and disaggregation assays, both L1 and L2 have an effective protection on Aβ_{40} aggregates. The ThT fluorescence spectra of Aβ_{40} with or without L1 or L2 for 1 to 3 days are shown in Figure S3. The addition of L1 or L2 to Aβ_{40} did not shift the ThT fluorescence spectra dramatically. Taken together, the results from BCA protein assay and ThT fluorescence assay further support that L1 and L2 are capable of inhibiting and

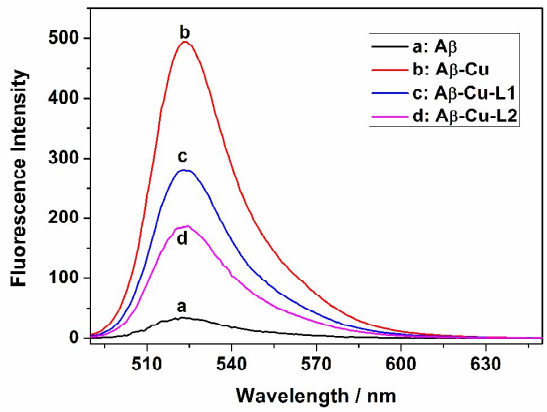

Fig. 5 Fluorescence of DCF reflecting the effect of L1 and L2 on the production of H_2O_2 by Cu- Aβ_{40} complex (([Aβ_{40}] = 300 nM, [Cu^{2+}] = [chelator] = 150 nM, [HRP] = 0.03 μM, [DCFH] = 100 μM, [ascorbate] = 2 μM, pH = 7.4).

disassembling the metal-induced Aβ_{40} aggregation by chelating metal ions from metal-Aβ_{40} aggregates rather than the interaction of Aβ_{40} and L1/L2, and metal chelation by L1 and L2 play a major role in modulation of metal-induced Aβ_{40} aggregation.

Conformational Reconversion of Aβ_{40}

To investigate the effect of L1 and L2 on the Zn^{2+}-and Cu^{2+}-induced conformational transition of Aβ_{40}, circular dichroism was applied to observe the changes in secondary structures of Aβ_{40}. Aβ_{40} incubated alone produced random coil conformation as revealed in its far UV-CD spectrum (Figure 4).[46]Incubation of Aβ_{40} with Zn^{2+} or Cu^{2+} generated a characteristic far-UV CD spectrum for *β*-sheet structure with a minimum ellipticity around 216 nm (Figure 4). CD data show that the addition of Zn^{2+}/Cu^{2+} to Aβ_{40} induced a *β*-sheet conformation consistent with the metal effects on *β*-aggregation monitored by ThT fluorescence. A conformational shift from random coil to a *β*-sheet structure is necessary for A*β* fibril formation.[25, 47] All three histidine residues of A*β* are involved in the interaction with metal ions, and the metal-His(Nτ) ligation is a common feature among the insoluble Zn^{2+}- and Cu^{2+}-Aβ_{40} aggregates. *β*-sheets of A*β* are crosslinked with His(Nτ)-metal-His(Nτ) bridges.[48] After L1 or L2 was added to the Zn^{2+}- or Cu^{2+}-Aβ_{40} solution, the spectrum typical of the random coil conformation reappears. L1 and L2 can coordiante with Zn^{2+} or Cu^{2+} from the Zn^{2+}/Cu^{2+}-Aβ_{40} complex, then both Zn and Cu are released from the Nτ atom and the breakage of the metal-His(Nτ) bond leads to the recovery of the Aβ_{40} conformation. Thus, L1 and L2 can not only resolubilize metal-Aβ_{40} aggregates, but also can reconvert Aβ_{40} conformation from *β*-sheet to random coil, which imply that L1 and L2 may have therapeutic potential in the treatment of AD.

Inhibition of H_2O_2 Production

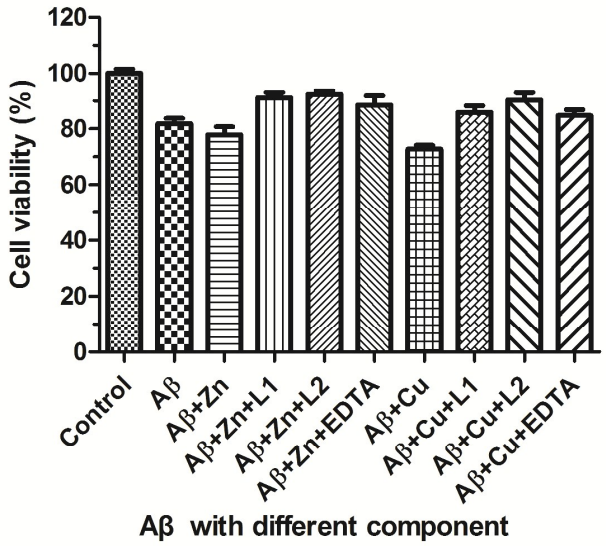

Fig. 6 Cell viability (%) of Aβ_{40} in the absence or presence of metal ions and chelaors toward SH-SY5Y cells tested by the MTT assay ([Aβ_{40}]= 10 μM; [Aβ_{40}] : [Cu^{2+}]/ [Zn^{2+}]: [L1]/ [L2]/[EDTA] = 1 : 2 : 4).

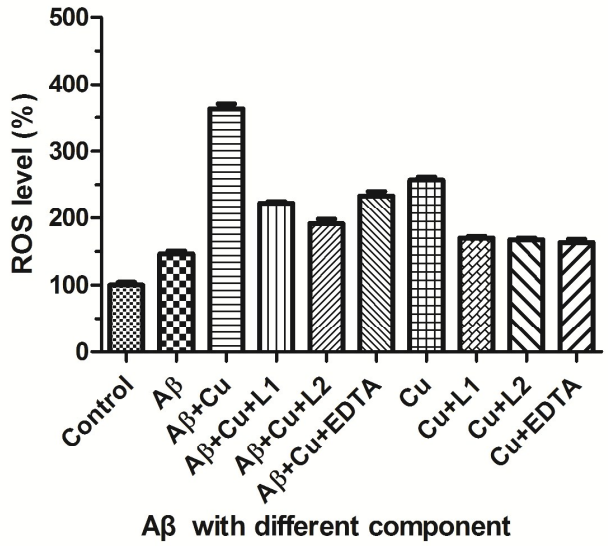

Fig. 7 ROS levels in SH-SY5Y cells upon treatment with Aβ_{40} in the absence or presence of metal ions and chelaors ([Aβ_{40}]= 10 μM; [Aβ_{40}] : [Cu^{2+}]/ [Zn^{2+}]: [L1]/ [L2]/[EDTA] = 1 : 2 : 4). ROS level (%) depicted in the figure is relative to the generation of control.

Redox-active metal ions such as Cu and Fe ions have been shown to promote Aβ aggregation, leading to the formation of ROS (e.g. H_2O_2) and inducing oxidative stress associated with Aβneurotoxicity.[49, 50] In our work, the effect of L1 and L2 on the Cu^{2+}-Aβ_{40}-mediated H_2O_2 generation was investigated by a DCF assay. DCF is a fluorescent marker derived from the reaction of nonfluorescent 2′,7′-dichlorofluorescin (DCFH) with H_2O_2 in the presence of horseradish peroxidase (HRP), which can indirectly indicate the generation of H_2O_2 from the Cu^{2+}-Aβ_{40} complex.[51] As shown in Figure 5, the fluorescence intensity of DCF is quite strong for Cu^{2+}-Aβ_{40} system without compounds, but in the presence of L1 and L2, the fluorescence intensity about decreased by 42.9 % and 63.3 %, respectively. The affinity of L1 and L2 for Cu^{2+} is sufficient to dissociate low-affinity bound Cu^{2+} from Aβ_{40} and the results indeed show that L2 is more efficient than L1. In addition, Cu^{2+}-Aβ_{40}-mediated redox activity might also be blocked by the formation of complexes with L1 and L2. Overall, these results support that L1 and L2 can not only facilitate metal-mediated disaggregation of Cu^{2+}-Aβ_{40} aggregates, but also can lower H_2O_2 production induced by Cu^{2+}-Aβ_{40} complex, which showed promise for their future applications.

Attenuation of Aβ_{40} Neurotoxicity

Metal-associated Aβ species in living cells are suggested to be neurotoxic. We examine the neuro-protective properties of L1 and L2 toward metal-Aβ40-induced toxicity in SH-SY5Y cells by the MTT assay. First, the cytotoxicity from the cells treated with Aβ40 and either Zn^{2+} or Cu^{2+} in the absence of L1 and L2 was investigated. As indicated in Figure 6, 77.8 % and 72.7 % of cells incubated with Zn^{2+}- and Cu^{2+}- treated Aβ_{40} for 24 h survived, respectively, compared to 81.9 % of those treated with metal-free Aβ_{40}. Secondly, to investigate the effect of L1 or L2 on metal-Aβ_{40} neurotoxicity in living cells, cells were introduced with Aβ_{40} and metal ions immediately followed by L1 or L2. Noticeably, 24 h treatment of L1 or L2 with cells including Aβ_{40} and either Zn^{2+} or Cu^{2+} presented better cell survial (91.1 % and 92.4 % for Zn^{2+}- Aβ_{40}; 86.0 % and 90.3 % for Cu^{2+}-Aβ_{40}). L1 and L2 can alleviate the neurotoxicity of Cu^{2+}-Aβ_{40} species. Furthermore, the cytotoxicity of L1 or L2 in the presence of of Zn^{2+} or Cu^{2+} was examined in SH-SY5Y cells. More than 95 % cell survival was observed from cells treated with metal-chelator complexes (Figure S5), which suggest that the toxicity under discussion mainly arises from the metal-Aβ_{40} aggregates. A similar cell survival about 86.0 % was observed for Aβ_{40} in the absence or presence of L1/L2 (Figure S4), indicating that L1 and L2 have little effect on the cells treated with Aβ_{40}. We aslo employed conventional chelator ethylenediaminetetraacetic acid (EDTA) as control group. The ability of L1 and L2 to inhibit Zn^{2+}- or Cu^{2+}- induced Aβ_{40} neurotoxicity is better than that of EDTA and L2 seems to be more efficient than L1. Over all, our study suggests that both L1 and L2 may regulate metal-induced Aβ_{40} neurotoxicity in living cells, which is expected based on their reactivity in vitro (anti-Aβ_{40} aggregation as well as ROS regulation).

Suppression of Intracellular ROS

In our work, the ROS levels in SH-SY5Y cells upon treatment with Aβ_{40} or Cu- Aβ_{40} in the presence or absence of L1 or L2 were detected by DCFH-DA assay. DCFH-DA (dichlorofluorescin-diacetate) was used as a probe for intracellular ROS because it diffuses into cells and becomes fluorescent DCF (dichloro-fluorescin) via oxidation by intracellular ROS.[52] As shown in Figure 7, treatment with Aβ_{40} for 24h promoted the ROS production in SH-SY5Y cells by 1.47-fold compared with control. Exposure of the cells to Cu-Aβ_{40} complex dramatically promoted the generation of ROS,

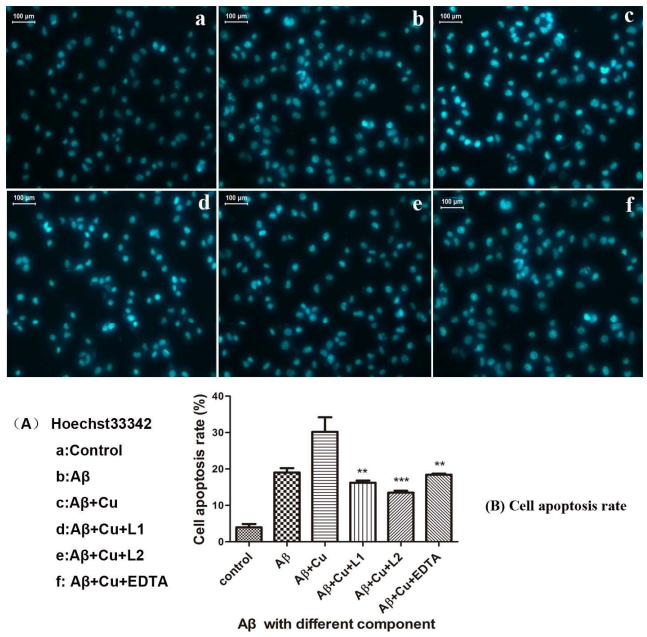

Fig. 8 Effect of L1 and L2 on the cell apoptotic induced by Cu-Aβ_{40} using Hoechst 33324 staining assay in SH-SY5Y cells. (A) Representative photomicrographs of cultured SH-SY5Y cells showing the apoptosis of control(a), Aβ_{40}(b), Cu-Aβ_{40}(c), L1-Cu-Aβ_{40}(d), L2-Cu-Aβ_{40}(e); EDTA-Cu-Aβ_{40}(f) (B) Cell apoptosis rate. Data expressed as mean ± SEM (n=3). $^{**}p < 0.01$, Cu-Aβ_{40} vs L1-Cu-Aβ_{40}; $^{***}p < 0.01$, Cu-Aβ_{40} vs L2-Cu-Aβ_{40}; $^{**}p < 0.01$, Cu-Aβ_{40} vs EDTA-Cu-Aβ_{40}.

with 3.63-fold increases relative to the control. Cu-Aβ_{40} aggregates induced ROS generation mainly via the redox cycling of copper ions by the Fenton-type and Haber-Weiss-type reactions.[42] However, treatment of the cells with L1 or L2 caused levels of ROS to diminish by 38.7 % and 47.3 %, respectively, compared to cells exposed only to Cu-Aβ_{40}. Compared with EDTA, L1 and L2 significantly decreased intracellular ROS production caused by Cu-Aβ_{40} complex. The results revealed that L1 and L2 showed good protection against the Aβ_{40} neurotoxicity. Furthermore, ROS generation caused by Cu^{2+} in cells also can be reduced by 33.8 % and 34.8 % in the presence of L1 and L2, respectively. We noted that L2 is capable of reducing ROS production to the great extent, thus resulting in the most effective protective capacity. On the one hand, we attribute this to the chelator composition itself. Pyridine containing analogs have long been reported in the literature to be potent antioxidants, which is attributed to the electron deficient nature of the pyridine. ring. Pyridine based compounds are known to produce N-oxides upon incubation with H_2O_2.[41] L2 has two pyridine rings while L1 has one pyridine ring, so L2 shows a superior antioxidant activity. On the other hand, L1 and L2 have antioxidant capacity in that L1 and L2 could inhibit the redox activity of the Cu^{2+} bound to Aβ_{40}. The inhibition of metal-mediated ROS production from Aβ_{40} by L1 and L2 could, therefore, facilitate Aβ_{40} clearance mechanisms.

Protection against Cell Apoptosis

The nuclear Hoechst 33342 staining assay in Aβ_{40}-treated cells was performed to evaluate apoptosis. As shown in Figure 8(A), the cells treated with Aβ_{40} or Cu^{2+}-Aβ_{40} showed typical characteristics of apoptosis, including the condensation of chromatin, shrinkage of nuclear and the appearance of a few apoptotic bodies, whereas the control culture had round blue nuclei of viable cells. However, with L1 or L2 pretreatment, the number of cells with nuclear condensation and fragmentation was markly decreased. The proportion of apoptotic cells was calculated as shown in Figure 8(B). The percentage of apoptotic cells induced by Aβ_{40} or Cu^{2+}-Aβ_{40} was 19.0 % and 31.2 % , respectively, compared with no Aβ_{40} or Cu^{2+}-Aβ_{40} of untreated control cells. While in the presence of 10 μM L1 or L2, cell apoptosis was decreased noticeably to 16.2 % and 13.5 %, respectively. By comparison, a slightly stronger ability of L2 than L1 to regulate the injury of Cu^{2+}-induced Aβ_{40} aggregation was observed, indicating that L2 can effectively interfere with the Aβ_{40}-induced intracellular injury. This result is consistent with suppression of intracellular ROS studies discussed above. Overall, this observation manifests that L1 and L2 can protect SH-SY5Y cells from apoptosis exerted by the injury of Cu^{2+}-induced Aβ_{40} aggregation and oxidative stress.

4. Conclusion

AD is a complex multifactorial syndrome unlikely to arise from a single causal factor. Different number of related biological alterations may contribute to AD pathogenesis. None of the presently marketed drugs, although valuable in improving cognitive, behavioral, and functional impairments, can alter AD progression. Metal ions such as Zn^{2+} and Cu^{2+} are involved in the assembly and neurotoxicity of Aβ_{40} species. It has been considered that modulating metal ion homeostasis via metal chelation therapy may be a valid method to control the onset of AD. In this regard, we have studied the effect of macrocyclic polyamine cyclam derivatives on the Aβ_{40} aggregation induced by Zn^{2+} and Cu^{2+}. These chelators exhibit the capability to inhibit the metal-mediated Aβ_{40} aggregation and disassemble performed Aβ_{40} aggregates. They also prevent the formation of the β-sheet structure and promote the reversion of the β-sheet to the normal random coil conformation. Moreover, they can dramatically reduce H_2O_2 formation by Cu-Aβ_{40} species, thus exhibiting also an antioxidant functionality. Interestingly, L1 and L2 can attenuate Zn^{2+}- or Cu^{2+}-Aβ_{40}-induced neurotoxicity, suppress the intracellular ROS and protect against cell apoptosis. Moreover, the tests for neurotoxicity, ROS generation, and cell apoptosis indeed show that L2 is more efficient than L1. Structural is the molecular basis of drug action. L2 bears two pyridine rings, while L1 has one pyridine ring, and hence a difference in inhibitory efficacy is expected between them. L2 performed a stronger antioxidant capacity than L1. These preliminary findings indicate that L1 and L2 have promising perspective of application in the treatment of AD, and therefore deserve further investigation as potential anti-AD agents. In our future efforts, we intend to extend this work and build a foundation toward the development of chemical tools for uncovering complex AD pathogenesis that

will form the basis for the discovery of effective therapeutics for this disease.

We greatly appreciate the support of the National Natural Science Foundation of China (21201105, 21203103), Natural Science Foundation of Jiangsu Province (BK20131200), Natural Science Foundation of Jiangsu Higher Education Institutions of China (12KJB150019), Natural Science Foundation of Nantong City (BK2012012, BK2014071), the Priority Academic Program Development of Jiangsu Higher Education Institution (PAPD) and Graduate Innovative Project of Nantong University (YKC 14073). This work is also sponsored by Qing Lan Project of Jiangsu Province and Innovation Found of Nantong University.

Notes and references

[a] *School of Chemistry and Chemical Engineering, Nantong University, Nantong, 226019, P. R. China*
[b] *Institute of Nautical Medicine, Nantong University, Nantong, 226019, P. R. China*
[c] *Department of General Surgery, Affiliated Hospital of Nantong University, Nantong, 226001, P. R. China*
[d] *Co-innovation Center of Neuroregeneration, Nantong University, Nantong, Jiangsu 226001, P. R. China*
****Corresponding author***
Dr. Tingting Chen
School of Chemistry and Chemical Engineering, Nantong University, 9 Seyuan Rd, Nantong 226019, P. R. China.
E-mail: tingtingchenntu@163.com(T.T. Chen)
Prof. Dr. Li Zhu
Institute of Nautical Medicine, Nantong University, 9 Seyuan Rd, Nantong, 226019, P. R. China
E-mail: lzhu1965@163.com (L. Zhu)

1. M.P. Mattson, *Nature*, 2004, **430**, 631-639.
2. R. Jakob-Roetne and H. Jacobsen, *Angew. Chem. Int. Ed.*, 2009, **48**,3030-3059.
3. I. W. Hamley, *Chem. Rev.*, 2012, **112**, 5147-5192.
4. K. P. Kepp, *Chem. Rev.*, 2012, **112**, 5193-5239.
5. M. G. Savelieff, S. Lee, Y. Liu and M. H. Lim, *ACS Chem. Biol.*, 2013, **8**, 856-865.
6. L. E. Scott and C. Orvig, *Chem. Rev.*, 2009, **109**, 4885-4910.
7. E. Gaggelli, H. Kozlowski, D. Valensin and G. Valensin, *Chem. Rev.*,2006, **106**, 1995-2044.
8. K. S. Kosik, *Science*, 1992, **256**, 780-783.
9. J. A. Hardy and G. A. Higgins, *Science*, 1992, **256**, 184-185.
10. J. Hardy and D. J. Selkoe, *Science*, 2002, **297**, 353-356.
11. A. S. Pithadia and M. H. Lim, *Curr. Opin. Chem. Biol.*, 2012, **16**, 67-73.
12. Y. Miller, B. Ma and R. Nussinov, *Chem. Rev.*, 2010, **110**, 4820-4838.
13. C. Haass and D. J. Selkoe, Nat. Rev. *Mol. Cell Biol.*, 2007, **8**, 101-112.
14. G. M. Shankar, S. Li, T. H. Mehta, A. Garcia-Munoz, N. E. Shepardson, I. Smith, F. M. Brett, M. A. Farreel, M. J. Rowan, C. A. Lemere, C. M. Regan, D. M. Walsh, B. L. Sabatini and D. J. Selkoe, *Nat. Med.*, 2008, **14**, 837-842.
15. P. Faller, C. Hureau, *Dalton Trans.*, 2009, **7**, 1080-1094.
16. M. A. Lovell, J. D. Robertson, W. J. Teesdale, J. L. Campbell and W. R. J. Markesbery, *Neuro. Sci.*, 1998, **158**, 47-52.
17. K. J. Barnham, C. L. Masters and A. I. Bush, *Nat. Rev. Drug Discovery*, 2004, **3**, 205-214.
18. A. I. Bush, *Neurobiol. Aging*, 2002, **23**, 1031-1038.
19. P. Faller, *ChemBioChem*, 2009, **10**, 2837-2845.
20. P. Zatta, D. Drago, S. Bolognin and S. L. Sensi, *Trends Pharmacol. Sci.*, 2009, 30, 346-355.
21. A. Rauk, *Chem. Soc. Rev.*, 2009, **38**, 2698-2715.
22. J. W. Karr, L. J. Kaupp and V. A. Szalai, *J. Am. Chem. Soc.*, 2004, **126**, 13534-13538.
23. A. I. Bush, *Trends Neurosci.*, 2003, **26**, 207-214.
24. A. Rauk, *Dalton Trans.*, 2008, **10**, 1273-1282.
25. X. D. Huang, C. S. Atwood, M. A. Hartshorn, G. Multhaup, L. E. Goldstein, R. C. Scarpa, M. P. Cuajungco, D. N. Gray, J. Lim and R. D. Moir, *Biochemistry*, 1999, **38**, 7609-7616.
26. J. Alí-Torres, L. Rodríguez-Santiago, L. Sodupe and L. A. Rauk, *J. Phys. Chem. A,* 2011, **115**, 12523-12530.
27. L. Guilloreau, S. Combalbert, A. Sournia-Saquet, H. Mazarguil and P. Faller, *ChemBiochem*, 2007, **8**, 1317-1325.
28. C. Migliorini, E. Porciatti, M. Luczkowski, D. Valensin, Coord. *Chem. Rev.*, 2012, **256**, 352-368.
29. J. H. Viles, *Coord. Chem. Rev*., 2012, **256**, 2271-2284.
30. D. J. Hayne, S. Lim and P. S. Donnelly, *Chem. Soc. Rev.*, 2014, **43**, 6701-6715.
31. L. E. Scott, C. Orvig, *Chem. Rev.*, 2009,**109**,4885-4910.
32. A. I. Bush and R. E. Tanzi, *Neuro therapeutics*, 2008, **5**, 421-432.
33. T. T. Chen, X. Y. Wang, Y. F. He, C. L. Zhang, Z. Y. Wu, K. Liao, J. J. Wang and Z. J. Guo, *Inorg. Chem.*, 2009, **48**, 5801-5809.
34. A. M. Mancino, S. S. Hindo, A. Kochi and M. H. Lim, *Inorg. Chem.*, 2009, **48**, 9596-9598.
35. D. R. C. McLachlan, A. J. Dalton, T. P. Kruck, M. Y. Bell, W. L. Smith, W. Kalow and D. F. Andrews, *Lancet*, 1991, **337**, 1304-1308.
36. C. W. Ritchie, A. I. Bush, A. Mackinnon, S. Macfarlane, M. Mastwyk, L. MacGregor, L. Kiers, R. Cherny, Q. X. Li, A. Tammer, D. Carrington, C. Mavros, I. Volitakis, M. Xilinas, D. Ames, S. Davis, K. Beyreuther, R. E. Tanzi and C. L. Masters, *Arch. Neurol*., 2003, **60**, 1685-1691.
37. L. Lannfelt, K. Blennow, H. Zetterberg, S. Batsman, D. Ames, J. Harrison, C. L. Masters, S. Targum, A. I. Bush, R. Murdoch, J. Wilson and C. W. Ritchie, *Lancet Neurol.*, 2008, **7**, 779-786.
38. L. Cahoon, *Nat. Med.*, 2009, **15**, 356-359.
39. J. L. Arbiser, S.-K. Kraeft, R. Van Leeuwen, S. J Hurwitz, M. Selig, G. R. Dickersin, A. Flint, H. R. Byers and L. B Chen, *Mol. Med.*, 1998, **4**, 665-670.
40. C. Rodríguez-Rodríguez, M. Telpoukhovskaia, and C. Orvig, *Coord. Chem. Rev.*, 2012, **256**, 2308-2332.
41. K. M. Lincoln, T. E. Richardson, Lauren. Rutter, P. Gonzalez, J. W. Simpkins and K. N. Green, *ACS Chem. Neurosci.*, 2012, **3**, 919-927.
42. Z. H. Xu, Y. M. Zhang, Z.Q. Xue, X. L. Yang, Z. Y. Wu and Z. J. Guo, *Inorg. Chim. Acta*, 2009, **362**, 2347-2352.
43. X. D. Huang, C. S. Atwood, R. D. Moir, M. A. Hartshorn, J. P. Vonsattel, R. E. Tanzi, and A. I. Bush. *J. Biol. Chem*., 1997, **272**, 26464–26470.
44. X. Du, Z. Wang, Y. Zheng, H. Li, J. Ni and Q. Liu, *Inorg. Chem.*, 2014, **53**, 1672-1678.
45. J. H. Luo, C. H. Yu, H. X. Yu, R. Borstnar, S. C. L. Kamerlin, A. Gräslund, J. P. Abrahams and S. K. T. S. Wärmländе, *ACS Chem. Neurosci.*, 2013, **4**, 454-462.

46. A. K. Tickler, D. G. Smith, G. D. Ciccotosto, D. J. Tew, C. C. Curtain, D. Carrington, C. L. Masters, A. I. Bush, R. A. Cherny, R. Cappai, J. D. Wade and K. J. Barnham, *J. Biol. Chem.* 2005, **280**, 13355-13363.
47. C. S. Atwood, R. C. Scarpa, X. Huang, R. D. Moir, W. D. Jones, D. P. Fairlie, R. E. Tanzi and A. I. Bush, J. *Neurochem.* 2000, 75, 1219-1233.
48. T. Miura, K. Suzuki, N. Kohata and H. Takeuchi, *Biochemistry*, 2000, *39*, 7024-7031.
49. X. H. Wang, X. Y. Wang, C. L. Zhang, Y. Jiao and Z. J. Guo, *Chem. Sci*., 2012, **3**, 1304.
50. J. Geng, M. Li, L. Wu, J. Ren and X. Qu, *J. Med. Chem.*, 2012, **55**, 9146-9155.
51. C. Opazo, X. D. Huang, R. A. Cherny, R. D. Moir, A. E. Roher, A. R. White, R. Cappai, C. L. Masters, R. E. Tanzi, N. C. Inestrosa and A. I. Bush, *J. Biol. Chem.*, 2002, **277**, 40302-40308.
52. P. Shi, M. Li and J. S. Ren, *Adv. Funct. Mater.*, 2013, **23**, 5412-5419.